AIAA 80-0027R

Magnetohydrodynamics of Hypervelocity Pulsed Flows

D. A. Oliver,* T. F. Swean Jr.,† D. M. Markham,† and S. T. Demetriades‡
STD Research Corporation, Arcadia, Calif.

The magnetohydrodynamic behavior of shock-generated pulses of plasma ("plasmoids") in encounter with an applied magnetic field is studied. Reflection and transmission of the plasmoid shock front is revealed as well as the existence of Joule heated zones that are convectively unstable. It is shown that strong interaction plasmoids are not delimited by shock front and following contact surface; rather, they develop their own internal, evolving structure under the mutual influence of self-Joule heating, and induced magnetic field. As a result, the interaction zone behind an ionizing shock wave will decouple progressively from the shock front and follow a trajectory given by the particle motion of the gas rather than the wave motion of the shock front.

I. Introduction

IN the present work we study the behavior of shock-generated magnetohydrodynamic flow over the range of weak and strong magnetohydrodynamic interaction and low to high magnetic Reynolds numbers. Such a flow consists of a hot plasma "plasmoid" formed between a driven ionizing shock wave and its following contact surface. The plasmoid is created by a sudden release of energy in a driver section that is in contact with a test gas in which the plasmoid propagates. Such a flow may be driven, for example, by the use of focused chemical explosives.[1,2]

The conducting plasmoid enters a region in which an externally imposed magnetic field $\boldsymbol{B}_0$ and electrodes coupled to an external circuit exist (Fig. 1). The plasma conducts current to this external circuit and is subject to Lorentz forces and Joule heating as it propagates through the magnetic field. If the explosion drive is a chemical source, such a plasmoid will be of the order of 5-20 cm in length in traversing a magnetic field region of the order of 100 cm at velocities of the order of 10^4 ms^{-1}. The plasmoid may exist at pressures up to 1 k bar and energies of 5 eV.

If σ_0, ρ_0, U_0 are the characteristic electrical conductivity, mass density, and velocity within the plasmoid, the flow may be specified by an interaction number per unit length i and magnetic Reynolds number per unit length r_m (in addition to the gasdynamic Mach number).

$$i=\sigma_0 B_0^2/\rho_0 U_0 \qquad r_m=\mu_0\sigma_0 U_0 \tag{1a}$$

For an interaction region of length L, the nondimensional numbers are defined as

$$I\equiv\int_0^L i\,dx \qquad R_m\equiv\int_0^L r_m\,dx \tag{1b}$$

When $R_m \gg 1$, the appropriate measure of the interaction is the parameter S defined as

$$S\equiv (B_0^2/\mu_0)/\langle \rho U^2\rangle \tag{2}$$

where the spatial average $\langle\ \rangle$ is over the electrically conducting portion of the region L. For a uniform plasmoid of length a, these numbers become

$$I=\sigma_0 B_0^2 a/\rho_0 U_0, \quad R_m=\sigma_0\mu_0 U_0 a, \quad S=I/R_m$$

Pulsed magnetohydrodynamic flows have been examined in the case of low magnetic Reynolds number ($R_m \ll 1$) and weak interaction ($I \lesssim 1$).[3,4] Because of the low interaction, these studies revealed simple current flow through the plasmoid and weak magnetohydrodynamic deceleration.

The traverse ionizing shock wave that forms the front of the plasmoid has been extensively studied in the limit of infinitely large magnetic Reynolds number.[5-8] In addition to the exposition of the general Rankine-Hugoniot conditions for these shocks,[5] it has also been demonstrated that such shock waves can be reflected as well as transmitted upon encounter with an externally imposed magnetic field. These studies also showed that the electric field in front of the shock must be self-consistently determined with the dynamical state behind the shock and the electrical boundary conditions imposed upon the gas.[6]

In the present study, we examine the magnetohydrodynamics of the whole plasmoid in its encounter with, and transit through an externally imposed magnetic field. We show that under conditions of strong interaction, hypervelocity plasmoids can possess a rich variety of magnetohydrodynamic phenomena including magnetically reflected shock waves, embedded MHD discontinuities, and significant periods of transonic flow within the plasmoid. In particular, we reveal the dynamics of reflected and transmitted waves through the plasmoid in both the low and high magnetic Reynolds number regime. We reveal the behavior of electrothermally unstable plasmoids. We show that, in general, the plasmoid is not delimited by the region between the shock front and contact surface. Instead, the plasmoid develops its own internal, evolving structure governed by the mutual interaction of self-heating and induced self-fields.

Shock-generated hypervelocity flows of this kind are subject to a variety of nonideal phenomena. These include wall interaction effects (viscous losses, gas leakage, and ohmic voltage drops in boundary layers), thermal radiation losses, and kinetic/ionization relaxation effects behind shock waves. In the present study we ignore these effects and examine those phenomena which arise specifically from the magnetohydrodynamic interaction.

In Sec. II of what follows we present a mathematical description of the flow of quasi-one-dimensional plasmoids. In Sec. III we examine the dynamics of strong interaction plasmoids with an applied magnetic field but at low magnetic Reynolds number. In Sec. IV we similarly consider strong interaction plasmoids but at large magnetic Reynolds number. In Sec. V we illustrate the behavior of "transitional" plasmoids. These are flows in which the plasmoid enters the magnetic field at relatively low values of interaction parameter and magnetic Reynolds number. As a result of self-Joule heating, however, the plasmoid conductance is elevated as it progresses through the field carrying it into the strong interaction, high magnetic Reynolds number regime.

Presented as Paper 80-0027 at the AIAA 18th Aerospace Sciences Meeting, Pasadena, Calif., Jan. 14-16, 1980; submitted April 7, 1980; revision received Nov. 26, 1980.

*Vice President-Technical.
†Member, Senior Technical Staff.
‡Technical Director.

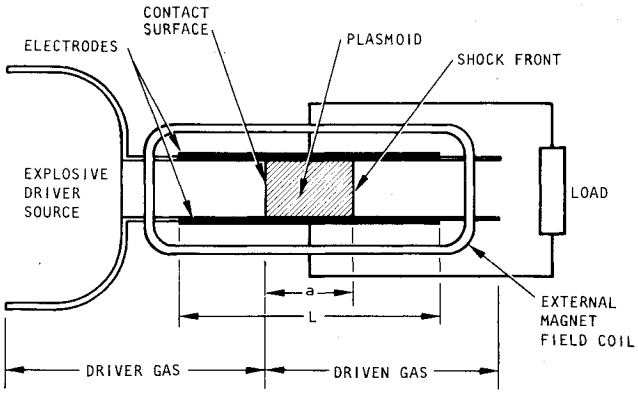

Fig. 1 Schematic of explosion driven plasmoid flow.

II. Mathematical Description

A. Conservation Laws for Fluid and Electricity

We consider a quasi-one-dimensional description of the gas moving over the spatial coordinate x in time t. Average properties (over the cross section) of the duct describing the flow are its density ρ, internal energy ϵ, velocity U, pressure p, and temperature T. The magnetic field $\boldsymbol{B}$ we separate into an applied field $\boldsymbol{B}_0$ and a field $\boldsymbol{B}_i$ induced by the plasma currents. From these we select the total mass, momentum, and energy densities

$$[\rho, m=\rho U, \quad e=\rho(\epsilon+U^2/2)]$$

as the state $W(x,t)$ specifying the flow at any point in space and time

$$W(x,t)=\begin{bmatrix}\rho\\ m\\ e\end{bmatrix} \tag{3}$$

The fluid conservation laws are

$$\frac{\partial W}{\partial t}=-\frac{\partial F}{\partial x}+\Xi \tag{4}$$

The conservation laws are augmented with equations of state

$$p=(\gamma-1)\rho\epsilon \qquad RT=p/\rho \tag{5}$$

where γ, R are taken as constants. In the above, $\boldsymbol{F}$ represents the convected fluxes of mass, momentum, and energy while Ξ contains the Lorentz force and power associated with the applied magnetic field and the Joule dissipation. These are expressed in terms of current density $\boldsymbol{J}$ and magnetic field $\boldsymbol{B}$

$$\boldsymbol{F}=\begin{bmatrix}m\\ m^2/\rho+p\\ m/\rho(e+p)\end{bmatrix} \quad \Xi=\begin{bmatrix}0\\ (\boldsymbol{J}\times\boldsymbol{B})_x\\ (\boldsymbol{J}\cdot\boldsymbol{E})\end{bmatrix} \tag{6}$$

In this illustration study we assume that the kinetic effects are confined to the relaxation layer at the shock, and further, that the relaxation layer is thin compared to the overall thickness of the plasmoid.

For the simple geometry (x,y,z) of Fig. 1, the magnetic field $\boldsymbol{B}$ is given by $\boldsymbol{B}(0,0,B_0)$, the electric field by $\boldsymbol{E}=\boldsymbol{E}(0,E,0)$, and the current by $\boldsymbol{J}=\boldsymbol{J}(0,J,0)$. The description for the near fields J, B_i of the plasmoid is then given by Ohm's law and the Maxwell equations in the MHD approximation

$$J=\sigma(E-UB_i-UB_0) \tag{7}$$

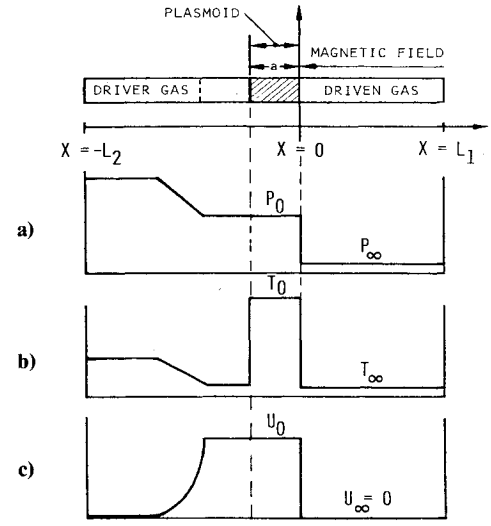

Fig. 2 Initial condition for plasmoid interaction for a) pressure, b) temperature, and c) velocity. Shock front of plasmoid of given breadth a, located at magnetic field edge at time $t=0$.

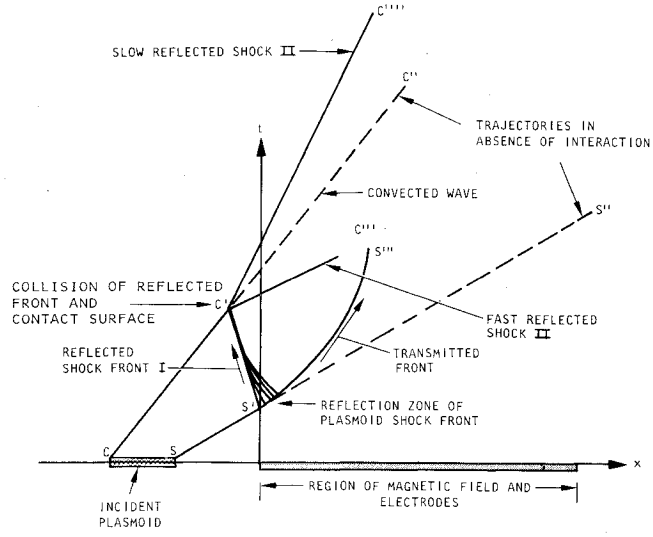

Fig. 3 Space-time diagram of strong interaction hypervelocity plasmoids. Plasmoid trajectory in the limit of vanishing interaction is delimited by the shock-front trajectory $SS'S''$ and contact surface trajectory $CC'C''$. Plasmoid shock-front reflection $S'C'$ and transmission $S'S''$ are initiated at encounter with magnetic field. Contact surface encounters reflected front at C' which generates fast reflected shock II ($C'C'''$), slow reflected shock II ($C'C'''$), and convected wave ($C'C''$).

$$\frac{\partial B_i}{\partial x}=-\eta(E-UB_i-UB_0) \tag{8}$$

where $\eta\equiv(\mu_0\sigma)^{-1}$ is the magnetic diffusivity.

External interaction conditions with an external circuit including inductive coupling with the applied magnetic field coil are required to complete the description of actual flow situations. Rather than include such circuit detail in these illustrations we assume that the external circuit is configured so that an electric field $E=E(0,E,0)$ is maintained within the interelectrode region whose magnitude is uniform in space and given by

$$E=\kappa\langle UB\rangle \tag{9}$$

where κ is a "load" parameter ($0\leq\kappa\leq 1$). For a passive external circuit, the value $\kappa=0$ corresponds to a shorted external circuit; for $\kappa=1$ the external circuit is open circuited.

The fluid variables ρ, p, T, σ, U are nondimensionalized by the values of $\rho_0, p_0, T_0, \sigma_0, U_0$ characterizing the interior of the

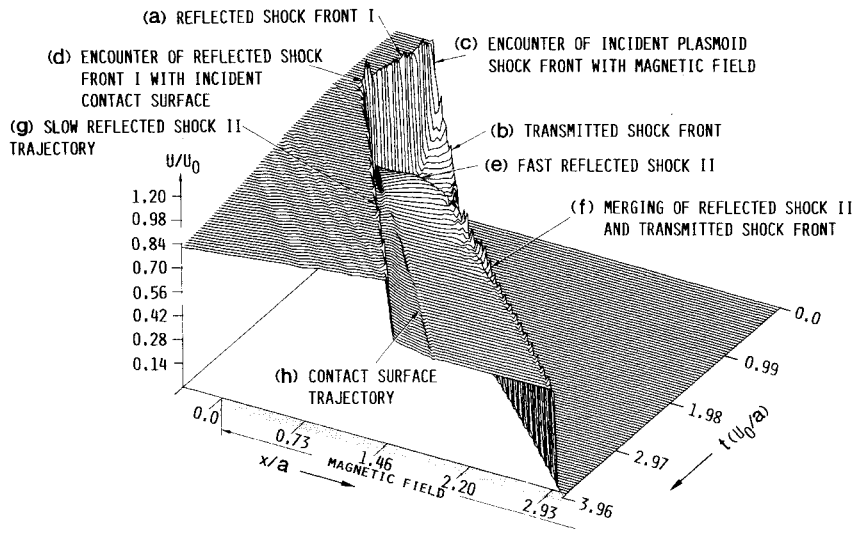

Fig. 4 Velocity field of plasmoid in transit through an applied magnetic field under strong interaction ($I=20$), low magnetic Reynolds number ($R_m=0.1$) conditions. Shock front of plasmoid is both reflected from magnetic field (a) and transmitted into magnetic field (b). Reflected wave I (a) collides with contact surface (d) and initiates a fast reflected shock II (e) and slow reflected shock (g). Reflected wave II (e) merges with transmitted shock front (f). Contact surface (h) separates conducting from nonconducting gas behind. Note transitory region of sharply diminished velocities within the plasmoid during the period of reflection and rereflection of the shock front.

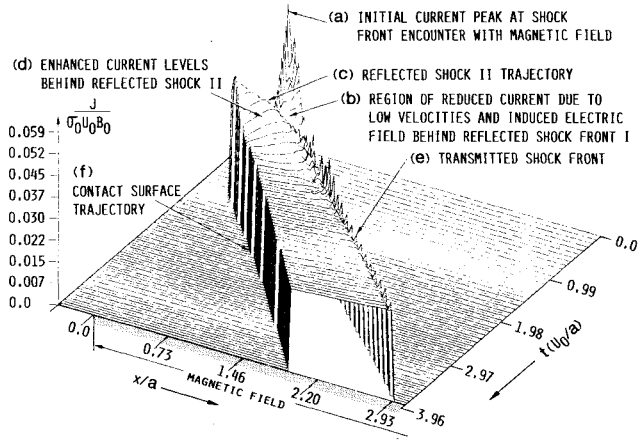

Fig. 5 Current density distribution for conditions of Fig. 4. Initial peak of current density (a) diminishes sharply as plasmoid velocities diminish behind reflected shock front I (b). After passage of reflected shock II (c) current levels rise (d) and remain uniform through plasmoid. With uniform conductivity model, conductivity is uniform between shock front (e) and contact surface (f). At low magnetic Reynolds number ($R_m=0.1$), current is diffused nearly uniformly over plasmoid.

Table 1 Conditions for interaction at low magnetic Reynolds number

$T_\infty \equiv$ Quiescent driven gas temperature	
$P_\infty \equiv$ Quiescent driven gas pressure	
$M=1.64$	$\gamma=1.5$
	$R_m=0.1$
$P_0/P_\infty=232$	$I=20$
	$S=200$
$T_0/T_\infty=45$	$\kappa=0.5$

initial plasmoid before encounter with the magnetic field. Nondimensional space and time $\bar{x}, \bar{t}$ are defined in terms of x, nondimensionalized by the plasmoid length a, and t by a/U_0. The nondimensional parameters governing the interaction are the Mach number M, the gas heat ratio γ, either of the interaction parameters I or S, and the magnetic Reynolds number R_m.

B. Boundary and Initial Conditions

In the limit of $R_m \to \infty$, the system consisting of Eqs. (4) and (7) and (18) is fully hyperbolic. For finite R_m, the system is mixed hyperbolic/parabolic with embedded regions where resistive effects occur. The boundary and initial conditions that specify the interaction problem for an explosion generated plasmoid encounter with a magnetic field are as follows. As an initial condition we take an idealized explosion driven flow in which the plasmoid of given breadth a occupies the hot zone between contact surface and shock front[9] (Fig. 2). At time $t=0$ the shock front is located at the edge of the magnetic field. Over the time scale for the dynamics of interest the shock front of the plasmoid will run continuously into the quiescent driver gas while the backward running rarefaction continuously runs into the explosive source. Hence the boundary conditions for the fluid equations are those of specified explosion and quiescent states at the boundaries $x=+L_1$, $x=-L_2$, respectively.

The boundary condition for the induced magnetic field B_i from Eq. (8) is that of symmetry across the overall plasmoid so that at $x=L_1$ and $x=-L_2$ which lie outside the region of any current flow

$$B_i(-L_2,t) = -B_i(L_1 t)$$

The applied magnetic field B_0 is uniform in both space and time.

C. Numerical Procedures

The solutions to the initial-value problems just formulated and to be discussed in Secs. III-V are computationally generated with second-order accurate explicit finite-difference operators. The hyperbolic system is treated with the MacCormack version of the Lax-Wendroff-Richtmyer operator.[10] For the space-time grid utilized, comparisons were made with the analytically available solutions for the zero and infinite R_m, zero interaction limits. At the extreme pressure ratios of 10^5 between driver and driven gas for these explosion generated plasmoids, the maximum variations between the computationally generated and analytical solutions within the plasmoid (expressed as a fraction of the analytical solution) are 0.025 in velocity, 0.04 in pressure, and 0.08 in temperature.

III. Interaction at Low Magnetic Reynolds Number

We now proceed to the first of several illustrations of the foregoing description. We consider first the strong interaction of a plasmoid with the magnetic field but at low magnetic Reynolds number. In Fig. 3 the kinematics of this situation are shown. When the incident plasmoid encounters the magnitude field, the leading shock front may be both transmitted and reflected. In the case of reflected fronts, the rear (contact surface) of the plasmoid subsequently interacts with the reflected shock front. This colliding disturbance then radiates a fast and slow reflected shock (denoted shock II)

back through the plasmoid (which consists of subsonic flow behind the reflected shock front) where it then collides with the now strongly decelerated shock front.

For the illustration shown here, we select a plasmoid with Mach number $M=1.64$, interaction parameters $I=20$, $S=200$, and Reynolds number $R_m=0.1$, just before encountering the magnetic field. The full conditions for the flow are given in Table 1. We impose the condition that the electrical conductivity is spatially uniform within the high temperature plasmoid (we consider electrical conductivity functions which are consistently coupled to the gas thermodynamic state in Sec. V). This uniform conductivity distribution is achieved in the computations with the model conductivity function

$$\sigma=0, \quad T/T_0<1/3$$

$$\sigma=\sigma_0, \quad T/T_0\geq 1/3$$

Table 2 Conditions for interaction at high magnetic Reynolds number

$M=1.64$	$\gamma=1.5$
	$R_m=5$
$P_0/P_\infty=232$	$I=20$
	$S=4$
$T_0/T_\infty=45$	$\kappa=0.5$

which effectively switches on a constant conductivity σ_0 within the plasmoid and switches the conductivity off outside the zone in which the plasmoid exists. The dynamics of the interaction are exhibited in Figs. 4 and 5. When the plasmoid shock front encounters the magnetic field, it is both reflected and transmitted. The reflected shock I collides with the contact surface and initiates a fast reflected shock II and a slow reflected shock. The fast reflected shock II re-establishes high velocity flow through the plasmoid and re-encounters the transmitted shock front that has been decelerated. During this period of strong wave dynamics the current distribution within the plasmoid is strongly affected (Fig. 5). The current is diminished to very small values during the period of plasmoid deceleration behind the reflected shock I, and then returns back to enhanced levels after passage of the fast reflected shock II. The low magnetic Reynolds number of the plasmoid allows the current to diffuse nearly uniformly throughout its breadth.

IV. Interaction at High Magnetic Reynolds Number

We next consider the behavior of a uniform conductivity plasmoid in the high magnetic Reynolds number regime. For this case the incident plasmoid has an interaction parameter $I=20$ as in the previous illustration but a magnetic Reynolds number $R_m=5$. Correspondingly, the interaction number S has the reduced value $S=4$. The complete conditions for this flow are given in Table 2. The encounter of this plasmoid with

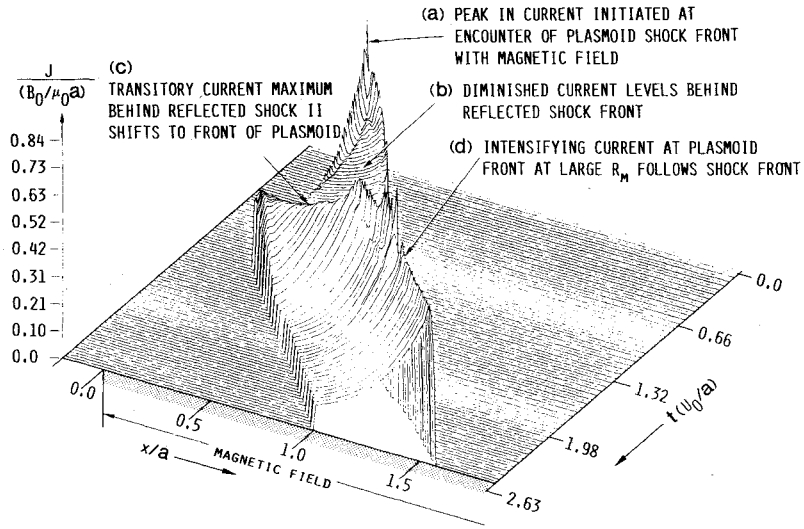

Fig. 6 Current distribution for a strong interaction plasmoid at $R_m=5$. Dynamics are similar to those exhibited in Figs. 4-6, however, the larger Reynolds number permits more nonuniform current (and induced magnetic field) distributions. Current pulse initiated by encounter of plasmoid shock front (a) gives way to diminished current levels in low velocity region behind reflected shock front I (b). Current levels rise and shift to front of plasmoid (c), (d) after passage of reflected shock front II. Note that current concentrates immediately behind shock front in contrast to that of Fig. 5 (where current is nearly uniform) and that of Fig. 8 (where current is nearly absent) behind shock front.

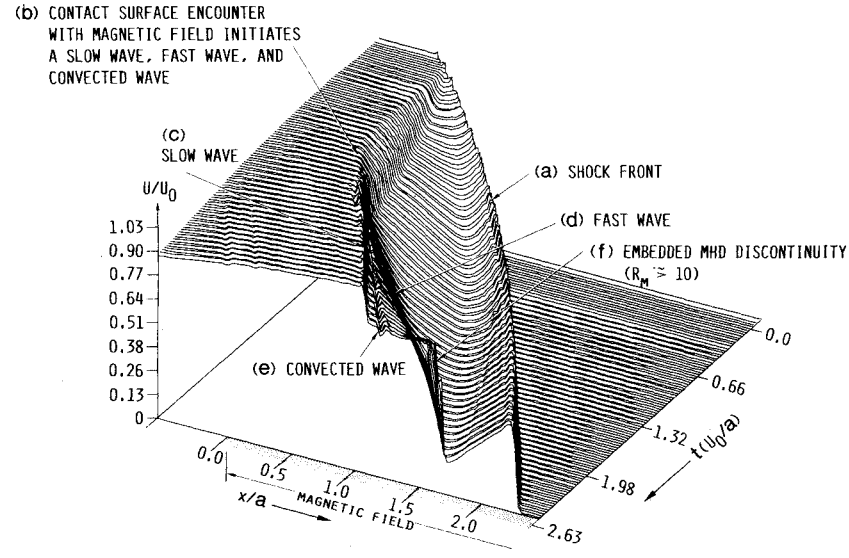

Fig. 7 Velocity distribution for a transitional plasmoid. Plasmoid enters magnetic field with $I=1$, $R_m=1$, and $S=1$. Modest interaction at entry to magnetic field does not generate distinct reflected waves, but rather strong and continuous deceleration. Magnetic Reynolds number and interaction parameters grow during the course of transit. Shock front proceeds through magnetic field with continuous deceleration (a). Once the Reynolds number reaches values $R_m \gtrsim 10$, the current has become sheet-like with a deflagration-like, intensifying discontinuity within a large subsonic zone of the plasmoid. Contact surface encounter with magnetic field (b) initiates downstream running waves (c), (d), (e).

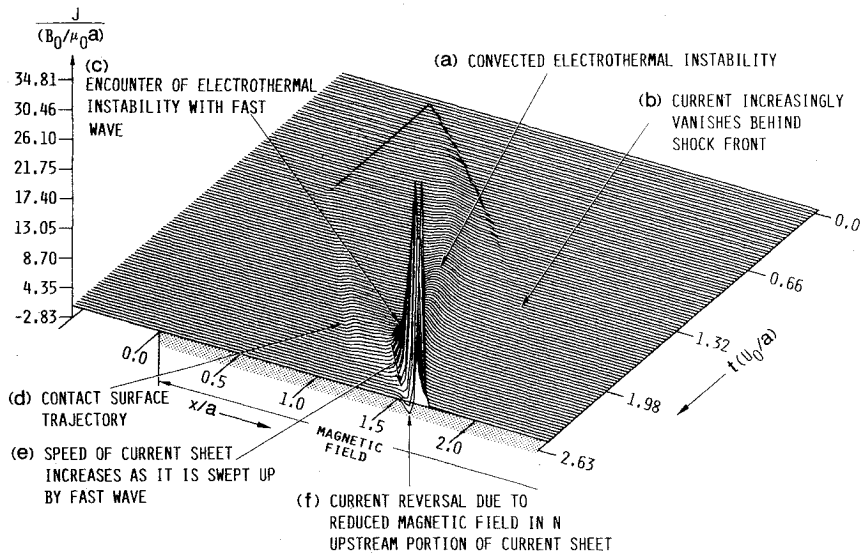

Fig. 8 Current distribution for transitional plasmoid of Fig. 7. Current concentration behind shock front at entry to magnetic field grows (a) with corresponding heating and conductivity enhancement (reflected in temperature field of Fig. 9). Shock front propagates ahead (b), but becomes increasingly free of current. Electrothermally heated zone becomes the most highly conducting region of the plasmoid. This heated zone is convected with the gas and strongly decelerated. Sharp rise in temperature and current occurs when unstably evolving current pulse (which is convected) collides with radiated wave (c). Current pulse is then swept up by contact surface and reaccelerated (e). Note current reversal due to sharply reduced magnetic field in upstream portion of current sheet (f).

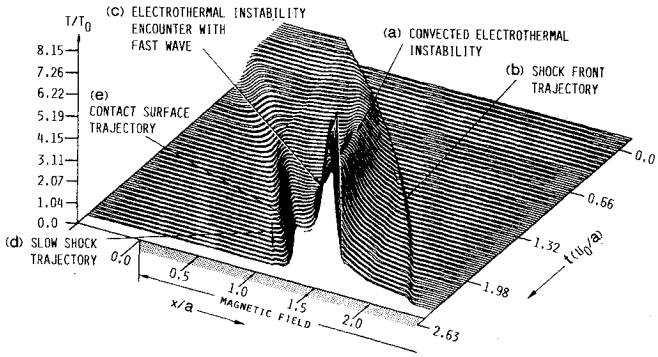

Fig. 9 Temperature field for transitional plasmoid corresponding to Figs. 7 and 8 showing developing electrothermal instability.

the magnetic field is similar to that of Sec. III. The features peculiar to the higher Reynolds number are best perceived in the current distribution of Fig. 6 which is more nonuniform compared to that of Fig. 5. When the current levels rise behind the reflected shock II, they do so by directly following the shock until it merges with the transmitted front. The current maximum then remains at the front of the plasmoid. As a result of decelerating Lorentz forces concentrated immediately behind the shock front, the front is slowed and the overall breadth of the plasmoid is decreased as it progresses through the magnetic field. This is in contrast to the plasmoid dynamics of Secs. III and V.

V. Transitional Plasmoids

We now turn to consideration of plasmoid behavior with a coupled electrical conductivity model. In contrast to the previous illustrations in which the conductivity is spatially uniform within the high temperature plasmoid and vanishes outside, we consider a conductivity that is appropriately coupled to the thermodynamic state of the gas. As a result, local regions within the plasmoid can be rendered more conductive by the self-Joule heating of the plasmoid. With the electrical conductivity strongly coupled to the Joule dissipation, a plasmoid in the low I, low R_m range can evolve into the large I, large R_m range as it progresses through the magnetic field and experiences further Joule heating. We term such flows "transitional" plasmoids.

We consider a conductivity function of the form

$$\sigma^{-1} = \sigma_{en}^{-1} + \sigma_{ei}^{-1} \tag{10}$$

In Eq. (10) σ_{en} is an electrical conductivity of a neutral species background and σ_{ei} is the Coulomb conductivity. We use as a

Table 3 Conditions for transitional plasmoid

$M=1.64$	$\sigma_0=1080$
$P_0/P_\infty=232$	$n=3.11$
$T_0/T_\infty=45$	$Z_{\text{eff}}^{-2}/\ell n\Lambda=0.16$
$\gamma=1.5$	$\kappa=0.5$
$R_m=1$	$I=1$
$S=1$	

summary representation of these two contributions the forms

$$\sigma_{en} = \sigma_0 (T/T_0)^n \tag{11}$$

$$\sigma_{ei} = 152 \bar{Z}_{\text{eff}}^{-2} T^{3/2}/\ell n\Lambda \tag{12}$$

where $\bar{Z}_{\text{eff}}$ is the average effective ionic charge and σ_0, T_0, $\ell n\Lambda$, $n>0$ are parameters for a given gas.

The conductivity function Eqs. (10-12) is dominated by the partially ionized conductivity σ_{en} at low temperature and goes over to the Coulomb (fully-ionized) conductivity at high temperature. This conductivity function has the property $\partial\sigma/\partial T \geq 0$ over the entire range of temperature. Since there are no thermal energy loss mechanisms (which would be principally radiative) included in the model, the plasmoid is unconditionally electrothermally unstable.[11,12] This convective instability is simply a growth of temperature nonuniformities within the plasmoid due to intensifying Joule heating resulting from growing electrical conductivity.

The interaction of a representative transitional plasmoid is shown in Figs. 7-9. This plasmoid has interaction parameters $I=1$, $S=1$, and magnetic Reynolds number $R_m=1$ just before it enters the magnetic field. The complete conditions for this flow are given in Table 3. It should be noted that the interaction at entry into the magnetic field is considerably smaller than the interaction described in Secs. III and IV. The plasmoid progresses into the field where it begins to self-heat and decelerate. The modest interaction at plasmoid entry to the magnetic field does not create distinct reflected waves, but rather a strong and continuous deceleration. Magnetic Reynolds number and interaction parameter grow significantly as the plasma is heated. At time $\bar{t}=2.6$, the magnetic Reynolds number is in excess of 10 and the current has become progressively sheet-like. It should be noted that the current maxima no longer follow immediately behind the transmitted shock front. Rather, the current concentrates in the electrothermally heated zone that is then convected at the local fluid speed rather than radiated at the shock front speed. This decelerating electrothermal instability is then swept up by collision with the waves initiated by the arrival of the contact

surface at the magnetic field inlet. A feature of note is the development of reversed current flow in the upstream portion of the current sheet due to the sharply diminished magnetic field behind the current sheet at large R_m.

VI. Summary Remarks

In this study we have illustrated significant purely magnetogasdynamic phenomena which occur when a hypervelocity pulse of plasma ("plasmoid") encounters an applied magnetic field under strong interaction conditions. With uniform electrical conductivity within the plasmoid (and vanishing electrical conductivity outside), reflection and transmission of the plasmoid shock front are possible coupled with strongly nonuniform current evolution in time. Such plasmoids with large magnetic Reynolds numbers have current distributions (and decelerating Lorentz forces) concentrated immediately behind the shock front. As a result of shock-front deceleration, these plasmoids diminish in breadth as they proceed through the magnetic field. With electrical conductivity within the plasmoid coupled to its thermodynamic state, the plasmoid is electrothermally unstable and creates its own, evolving region of enhanced electrical conductance which carries most of the current and is convected at the fluid speed within the plasmoid. The shock front becomes increasingly free of current and runs progressively farther ahead of the unstable current structure embedded in the plasmoid interior.

Nonideal phenomena such as viscous wall layers, kinetic-relaxation effects behind the shock front, and thermal radiation losses can play important roles in these strong interaction flows. The basic structure of the magnetohydrodynamic interaction itself, however, is a prerequisite to the description and understanding of these additional modifying effects.

Acknowledgment

This work was sponsored by the U.S. Office of Naval Research, Contract N00014-77-C-0574.

References

[1] Jones, M., "Explosion Driven Linear MHD Generators," *Proceedings of the Conference on Megagauss Magnetic Field Generation by Explosives,* Frescati, Italy, Sept. 1965.

[2] Glass, I. I., Chan, S. K., and Brode, H. L., "Strong Planar Shock Waves Generated by Explosively-Driven Spherical Implosions," *AIAA Journal*, Vol. 12, March 1974, p. 367.

[3] Rosciszewski, J. J. and Gallaher, W., "Shock Tube Flow Interaction with an Electromagnetic Field," *Proceedings of the Seventh International Shock Tube Symposium*, edited by I. I. Glass, Univ. of Toronto, 1970, pp. 475-489.

[4] Rosciszewski, J. J. and Yeh, T. T., "Shock Tube Flow Passing Through a Section of a Linear MHD Generator," *AIAA Journal*, Vol. 11, Dec. 1973, p. 1756.

[5] Chu, C. K. and Gross, R. A., "Shock Waves in Plasma Physics," *Adv. Pl. Phys.*, edited by A. Simon and W. B. Thompson, Vol. 2, 1969, p. 139.

[6] Chu, C. K., "Dynamics of Ionizing Shock Waves: Shocks in Transverse Magnetic Fields," *Physics of Fluids*, Vol. 7, Aug. 1964, p. 1349.

[7] Bout, D. A. and Gross, R. A., "Interaction of an Ionizing Shock Wave with a Transverse Magnetic Field," *Physics of Fluids*, Vol. 13, June 1970, p. 1473.

[8] Bout, D. A., Post, R. S., and Presby, H., "Ionizing Shocks Incident Upon a Transverse Magnetic Field," *Physics of Fluids*, Vol. 13, May 1970, p. 1399.

[9] Zel'dovich, Ya. B. and Raizer, Yu. P., *Physics of Shock Waves and High Temperature Hydrodynamic Phenomena*, Vol. 1, Academic Press, N.Y., 1966, pp. 234-238.

[10] Warming, R. F., Kutler, P., and Lomax, H., "Second- and Third-Order Noncentered Difference Schemes for Nonlinear Hyperbolic Equations," *AIAA Journal*, Vol. 11, Feb. 1973, pp. 196-204.

[11] Oliver, D. A., "A Constricted Discharge in Magnetohydrodynamic Plasma," *Proceedings of the 15th Symposium on Engineering Aspects of Magnetohydrodynamics*, Univ. of Pennsylvania, Philadelphia, Pa., May 1976, p. IX.4.

[12] Demetriades, S. T., Maxwell, C. D., Argyropoulos, G. S., and Fonda-Bonardi, G., "Influence of Controlled Turbulence on Gaseous Discharges," *Proceedings of the 11th Symposium on Engineering Aspects of Magnetohydrodynamics*, California Institute of Technology, Pasadena, Calif., March 1970, p. 64.